Macroscopic Torsional Strain and Induced Molecular Conformational Deracemization

Rajratan Basu, Joel S. Pendery, Rolfe G. Petschek, Robert P. Lemieux, and Charles Rosenblatt

Phys. Rev. Lett. **107**, 237804 — Published 2 December 2011

DOI: 10.1103/PhysRevLett.107.237804

Macroscopic torsional strain and induced molecular conformational deracemization

Rajratan Basu[a], Joel S. Pendery[a], Rolfe G. Petschek[a], Robert P. Lemieux[b], and Charles Rosenblatt[a]
[a]Department of Physics, Case Western Reserve University, Cleveland, Ohio 44106 USA
[b]Department of Chemistry, Queen's University, Kingston, Ontario K7L 3N6 Canada

A macroscopic helical twist is imposed on an achiral nematic liquid crystal by controlling the azimuthal alignment directions at the two substrates. On application of an electric field the director rotates in the substrate plane. This electroclinic effect, which requires the presence of chirality, is localized at the two substrates and increases with increasing imposed twist distortion. We present a simple model involving a tradeoff among bulk elastic energy, surface anchoring energy, and deracemization entropy that suggests the large equilibrium director rotation at the surfaces induces a deracemization of chiral conformations in the molecules, quantitatively consistent with experiment.

Chirality is ubiquitous in soft materials and plays a crucial role in a wide range of physical properties, from electrooptical to hierarchical and ultimately to long-range order. It is particularly important in liquid crystals (LCs), where many spectacular effects owe their existence to the absence of mirror symmetry. For example, the isotropic LC phase composed of chiral molecules exhibits an enormous increase in its optical rotatory power on cooling toward the orientationally ordered nematic (cholesteric) phase [1]. This is due to the increasing correlation length of the fluctuating (helical) nematic domains near the phase transition. In the mid-1970s Meyer, et al demonstrated the existence of a spontaneous electric polarization in a chiral smectic-*C** phase composed of chiral molecules [2]. With the advent Clark and Lagerwall's method of surface-stabilization to produce uniformly oriented cells [3], these so-called "ferroelectric liquid crystals" have been used in fast switching optical displays and light valves [4], and can be used as an alignment layer for electrically-controlled switching of the director orientation at a surface [5]. More than a dozen years ago Link, et al, demonstrated the existence of chiral smectic domains formed from bent-shaped, inherently achiral molecules, which in turn can give rise to macroscopic electric polarizations All of these chiral properties are "bottom-up" in nature, originating at the molecular level and resulting in macroscopic effects. In this paper we describe a "top-down" phenomenon, in which we apply a torsional strain to a nematic LC and observe a mechanoelectrical effect that normally is associated with local — even molecular level — chirality.

It is well known that chiral LC molecules, or even achiral molecules doped with a chiral agent, result in a macroscopic helical twist of the director $\hat{n}$ with a characteristic inverse pitch p_b^{-1} in the bulk that is sensitive to the molecular structure [6,7]. Such twisted, optically-birefringent helices can rotate the polarization of light and exhibit photonic band gaps. But a macroscopic twist structure also can be obtained from achiral molecules by control of the boundary conditions: The user-controlled "easy axes" for LC orientation at the two substrates of a cell need not be parallel or antiparallel, but can be set at some arbitrary angle θ_0 (Fig. 1), thereby resulting in a twist of $\hat{n}$ from one substrate to the other [8]. This is the architecture used in a "twisted nematic" LC display, where $\theta_0 \approx \pi / 2$. But such a twist creates local chiral symmetry, and in principle can induce a deracemization of chiral molecular conformations. In order to examine this deracemization we exploit the electroclinic effect (ECE), in which an applied electric field $\vec{E}$ induces a rotation of $\hat{n}$ from its equilibrium orientation by a small angle φ about the field axis when both chirality is present and the remaining symmetry is sufficiently reduced [9]. This effect was first observed in the smectic-*A* phase [9], but since has been observed in a bulk nematic phase (due to smectic fluctuations) [10] and in the nematic [11] and smectic-*A* [12] phases at a translational symmetry-breaking interface. Our central result is that, when a macroscopic helical twist is imposed, the ECE occurs principally at the substrate interfaces; its magnitude $e_c \equiv d\varphi/dE$ increases with decreasing pitch near the surface and is consistent with a simple model for conformational deracemization; and for opposite senses of twist, the phase of $d\varphi/dE$ with respect to the applied ac field differs by π.

Two wedged "twist cells" were prepared using indium-tin-oxide (ITO) coated glass substrates that were spin-coated with the planar-alignment agent RN-1175 polyamic acid (Nissan Chemical Industries). The coated substrates were baked for 60 min at 250 ^{o}C and rubbed unidirectionally using a cloth-covered rubbing wheel to establish easy axes for the director orientation. The two substrates were then placed together to form a wedge: They were separated by a Mylar spacer of nominal thickness 12.5 μm at one end and in contact at the other end, such that their rubbing directions were rotated by an angle $\theta_0 = (0.35 \pm 0.02)$ rad $= (20 \pm 1)^{o}$ with respect to each other (Fig. 1). Note that the ITO was etched off the glass at the narrow end of the wedge to prevent electrical contact between the substrates. Two such cells were fabricated, one having a right-handed (clockwise) 20^{o} rotation (Fig. 1) and the other a left-handed (counterclockwise) rotation. Both cells were filled with a negative dielectric anisotropy, achiral liquid crystal 9OO4 [Fig. 1, inset], which has a phase sequence Iso – 83° – N – 70° – Sm-*A* – 62° – Sm-*C* – 50° – Sm-*B* – 35° – Cryst.

The optical setup for the ECE experiments consisted of a beam from a 5-mW He-Ne laser at wavelength $\lambda = 633$ nm passing through a polarizer, the cell, an analyzer, and into a detector. The incoming polarizer was at an angle of $\pi/8$ clockwise (looking from the rear to the front of the cell, Fig. 1) with respect to the easy axis of the front substrate, and the analyzer was oriented at an angle of $-\pi/2-\theta_0$ and $-\pi/2+\theta_0$ relative to the polarizer for the right- and left-handed twist cells, respectively. θ_0 would be zero if there were no imposed twist, and the optical arrangement would correspond to the classical electroclinic geometry [13]. For $\theta_0 \neq 0$ the optical polarization approximately follows the relatively weak director twist (the Mauguin limit [8]) and the ordinary and extraordinary eigenmodes emerge from the cell rotated by $\pm\theta_0$, with the sign depending on the sense of the twist. Hence, assuming $\hat{n}$ is parallel to the easy axes, the orientations of the analyzer nearly maintain the classical electroclinic geometry [13]. The output of the detector was fed into both a dc voltmeter and a lock-in amplifier that was referenced to the driving frequency ν of the ac electric field E applied across the LC (Fig. 1). The ac intensity I_{ac}, its phase relative to E, and the dc intensity I_{dc} were computer recorded as E_{rms} was ramped upward with time over 500 s. Figure 2 shows $I_{\mathrm{ac}}/4I_{\mathrm{dc}}$ — this corresponds to φ in the classical electroclinic geometry [13] — at $\nu = 1000$ Hz at several thicknesses d, determined by interferometry, within the wedged cell.

To understand our results, we assume that the ECE is predominantly a surface effect for which the field induces a director rotation at the two surfaces that propagates elastically into the bulk; this surface hypothesis will be confirmed empirically. The two torque balance equations at the surfaces (of a right-handed twist cell) are $-K_{22}\left[\left(\theta_0+2\theta\right)/d\right]-W_2^{\varphi}\theta = CE$ and

$K_{22}\left[\left(\theta_0+2\theta\right)/d\right]+W_2^{\varphi}\theta=CE$ [14], where θ is the equilibrium twist-induced director *deviation* from the easy axes at the front of the cell when $E = 0$ (Fig. 1); K_{22} is the twist elastic constant; W_2^{φ} is the azimuthal anchoring strength coefficient, *i.e.,* the coefficient of the quadratic term in the surface free energy; and C is a material and temperature dependent parameter having units of charge per length. Thus $\theta=-K_{22}\theta_0/2\left(K_{22}+W_2^{\varphi}d/2\right)$ for $E = 0$. Using the very reasonable values $K_{22} = 2.5\times10^{-12}$ N [8] and $W_2^{\varphi} = 5\times10^{-6}$ J m^{-2} [15], we find $\theta \sim -2.5^{\circ}$ for $d = 3.2$ μm to $\sim -0.7^{\circ}$ for $d = 13.7$ μm. These are consistent with our polarizing microscope observations. From an optical standpoint, these deviations of $\hat{n}$ from the easy axes (Fig. 1) of a right-handed twist cell are the equivalent of a clockwise rotation of the polarizer by $|\theta|$ and counterclockwise rotation of the analyzer by $-|\theta|$ in an untwisted (classical electroclinic) cell. Thus, unlike the classic electroclinic geometry for which $\varphi = I_{\text{ac}}/4I_{\text{dc}}$ [13], the polarizer and analyzer no longer act as if they are crossed and the ratio $I_{\text{ac}}/4I_{\text{dc}}$ now depends on the total optical retardation γ ($\equiv 2\pi d\Delta n/\lambda$, where $\Delta n = 0.116$ is the birefringence measured at $T = 76$ °C in the nematic phase). For our typical values of K_{22}, W_2^{φ}, d, and Δn, it turns out that $\varphi = I_{\text{ac}}/4I_{\text{dc}}$ with an error well under 1% unless γ is close to an integer multiple 2π; details will be given elsewhere. All values of φ reported herein have been corrected for these angle and retardation effects.

The bulk behavior is described by the diffusion equation $\eta d\varphi/dt = K_{22}d^2\varphi/dz^2$ [14], where η is the twist viscosity. Accounting for the torque balance equations at the two surfaces, on application of field $E = E_0e^{-i\omega t}$ we obtain [14]

$$d\varphi/dE_0 = e_c\left(\omega\right) = Ce^{-i\omega t}/\left[W_2^{\varphi}+\sqrt{i\omega\eta K_{22}}\tanh\left(d\sqrt{i\omega\eta/K_{22}}/2\right)\right], \tag{1}$$

where $\omega = 2\pi\nu$ and $e_c^0 = C / W_2^\varphi$ is the dc electroclinic coefficient (at $\omega = 0$). Figure 2 inset shows the (γ-corrected) experimental magnitudes $|e_c(\omega)| = \left[\mathrm{Re}(e_c(\omega))^2 + \mathrm{Im}(e_c(\omega))^2\right]^{1/2}$ *vs.* ω for a region of the cell of thickness $d = 3.2$ μm. As the bulk nematic ECE [16] has much faster (sub-microsecond) response times, the sharp fall-off of $|e_c(\omega)|$ with ω clearly suggests a *surface* ECE that drags the bulk along elastically [11,14]. Noting in Fig. 2 inset that $|e_c(\omega)|$ decays from e_c^0 by a factor ~ 2 at $\omega \sim 200$ s^{-1}, we can use Eq. 1 to estimate the viscosity, finding $\eta \sim 0.05$ kg m^{-1} s^{-1}, a very typical value for nematic twist [17].

Let us now turn to our central result, the ECE as a function of the imposed helical twist. In obtaining $|e_c(\omega)|$ *vs.* ω (Fig. 2 inset) we found that, despite its much larger magnitude at low frequencies, the signal-to-noise level at low frequencies resulted in much larger relative errors. In consequence we chose to perform the experiment at $\nu_0 = 1000$ Hz, corresponding to $\omega_0 = 2\pi \times 1000$ s^{-1}. The effect of the higher frequency is to reduce the measured ECE by an approximately constant factor — note that the denominator in Eq. 1 is nearly independent of d for physically appropriate parameters — which allows us to compare the relative values of $|e_c(\omega_0)|$ for different helical pitches. Figure 3 shows $|e_c(\omega_0)|$ *vs.* cell thickness d, revealing several features. First, the ECE becomes small for large d, and was found to vanish identically when a non-twisted ($\theta_0 = 0$) cell was used; this is expected when the chirality vanishes. Second, the left- and right-handed twist cells yield similar magnitudes of the ECE. The differences in magnitude likely are due to local differences in W_2^φ and to small errors in thickness measurements. Additionally, and importantly, the inset in Fig. 3 shows that I_{ac} exhibits a relative phase difference of approximately π between the left- and right-handed cells, which is as expected from opposite handed helices. Taken as a whole, the data clearly show a mechanoelectrical effect, which is observed optically, due to a torsional strain on the LC.

We now speculate on the origin of this effect. Imposition of a macroscopic mechanical twist entails an elastic energy cost. With the approximation that there are only two enantiomeric conformers of equal energy in the ground state, *viz.*, right-handed (*P*) and left-handed (*M*), the elastic energy can be compensated in part by the induction of a conformational enantiomeric excess $\varepsilon \equiv ([P]-[M])/([P]+[M])$. But deracemization involves an entropy cost $F_{ent} = nk_BT\left[\left(\tfrac{1-\varepsilon}{2}\right)\log_e\left(\tfrac{1-\varepsilon}{2}\right)+\left(\tfrac{1+\varepsilon}{2}\right)\log_e\left(\tfrac{1+\varepsilon}{2}\right)\right]$, where $n = 1.4 \times 10^{21}$ cm^{-3} is the total number concentration of 9OO4, k_B is Boltzmann's constant, and T is temperature. On including the bulk twist and surface anchoring, the total free energy per volume is $F_{tot} = F_{ent} + \tfrac{1}{2}K_{22}\left[2\pi\beta_M\varepsilon-(\theta_0+2\theta)/d\right]^2 + \tfrac{1}{2d}W_2^{\varphi}\theta^2$. Here β_M is the helical twisting power of one of the enantiomers. For a typical chiral LC, $\beta_M \sim 50$ μm^{-1} [18]. It is important to realize that, once we allow for deracemization, the ground state chiral wavevector $q_c = 2\pi\beta_M\varepsilon$ also must appear inside the brackets in the two torque balance equations. This has the effect of reducing $|\theta|$ as ε increases, although it will turn out that ε is sufficiently small that these corrections can be neglected. On minimizing F_{tot} with respect to ε we find $\varepsilon = 2\pi\beta_M K_{22}(\theta_0+2\theta)/\left[d\left(4\pi^2\beta_M^2K_{22}+nk_BT\right)\right]$ for the induced enantiomer excess in the bulk. Using the parameters above, for a cell gap $d = 3$ μm we obtain $\varepsilon \sim 10^{-5}$ *in bulk*, sufficiently small to: i) justify neglecting the corrections due to ε and ii) render undetectable the bulk contribution to the nematic ECE, where $e_c \propto \varepsilon$. But we still need to treat the deracemization at the surfaces. Although the bulk pitch $p_b = 2\pi d/(\theta_0+2\theta) \sim 70$ μm for $d \sim 3$ μm, there is a much tighter effective pitch (or equivalently, an effective discontinuity) $p_s \sim -2\pi d_s/\theta$ at the surface, where the director rotates azimuthally by $-\theta$ over a small distance d_s ~ one to a few molecular diameters toward the surfaces' easy axes. Taking $\theta \sim -2.5^{\circ}$ for $d \sim 3$ μm and surface layer thickness $d_s \sim 2$ nm, we find $p_s \sim 0.3$ μm. The much tighter pitch at the surface suggests that the enantiomer excess ε_s *at the surface*, and thus the surface electroclinic response, would be of order p_b / p_s ~ 200 times larger than in the bulk. Thus, at the surface we can expect ε_s ~ 10^{-3}, where the surface is treated as a perturbation of the bulk, i.e., $d_s\varepsilon_s << d\varepsilon$. More generally, $|e_c(\omega_0)|$ would scale as $\varepsilon p_b / p_s \propto p_s^{-1} = -\Lambda\theta / 2\pi d_s = \Lambda K_{22}\theta_0 / 4\pi d_s \left(K_{22} + W_2^{\varphi} d / 2\right)$, where Λ is a constant that depends on K_{22}, n, and β_M. Thus, in Fig. 3 we perform a one parameter (Λ) fit of $|e_c(\omega_0)|$ *vs.* d to the form $\Lambda K_{22}\theta_0 / 4\pi d_s \left(K_{22} + W_2^{\varphi} d / 2\right)$; the fits are shown by lines, and suggest that the electroclinic response scales as p_s^{-1}.

The only extant experimental result for a surface ECE involving a fully chiral ($\varepsilon = 1$) LC at an achiral surface is by Maclennan, et al [12]. They obtained e_c^0 ~ 10^{-1} rad (V μm^{-1})$^{-1}$ in the smectic-*A* phase of the optically pure biphenyl benzoate W415*. If their enantiomer excess (at the surface) were instead ε_s ~ 10^{-3}, as is the case from our simple model, their value of e_c^0 would be ~ 10^{-4} rad (V μm^{-1})$^{-1}$, quantitatively consistent with our result (Fig. 2). Thus our results are consistent with, and strongly suggestive of, a deracemization mechanism at the surface. To be sure, a more fully developed model would include other effects at the surfaces, the multiplicity of conformational states, as well as the structural differences between our LC molecule and the surface alignment layer; effects linear in E that do not involve deracemization are difficult to adduce in this experimental geometry. All of these issues will be addressed elsewhere. Finally, we should be aware that direct comparisons of e_c^0 between different LCs and different phases can be treacherous. Nevertheless, the order of magnitude agreement suggests strongly that the spatially rapid equilibrium twist near the surface, which comes about as a consequence of the imposed macroscopic torsional strain and finite anchoring strength, results in a partial conformational deracemization of the LC. This is observed as a chirality-required surface electroclinic effect.

To summarize, we have demonstrated that an imposed helical twist in the nematic phase can result in a mechanoelectrical effect at a surface whose magnitude increases with decreasing helical pitch. We have presented a simple model that suggests the twist can induce a conformational enantiomeric excess, and argued that this deracemization can be much larger at the surfaces than in bulk. The resulting chirality near the surface is responsible for the observed effect.

Acknowledgments: R.B. and C.R. were supported by the U.S. Dept. of Energy's Materials Chemistry Program, J.S.P. by the National Science Foundation's Condensed Matter Physics and Solid State and Materials Chemistry Programs, and R.P.L. by a Discovery Grant from the Natural Sciences and Engineering Research Council of Canada.

Figures

Figure 1 Schematic diagram of experimental geometry for a right-handed twist cell. θ_0 is the rotation angle between the front and rear easy axes and θ is the deviation of the equilibrium director orientation $\hat{n}$ (dashed line) from the easy axis at the front substrate. Note that θ is negative for a right-handed twist. The electric field $\vec{E}$ is shown, and the laser light path runs from the front to the rear substrate. Analyzer is rotated counterclockwise from polarizer by an angle $-(\pi/2+\theta_0)$. Inset: Chemical formula for 9OO4.

Figure 2 The intensity ratio $I_{ac} / 4I_{dc}$ *vs.* applied voltage for five different cell widths *d* in the right-handed cell: Solid green triangles, 3.2 µm; solid red squares, 4.0 µm; solid orange circles, 5.1 µm; open blue diamonds, 8.5 µm; open black circles, 13.7 µm. The uncertainty in *d* is ± 0.2 µm. Inset: Electroclinic coefficient $e_c(\omega)$ *vs.* frequency at fixed voltage of 8 V_{rms} and $d = 3.2$ µm.

Figure 3 Electroclinic coefficient e_c at $\omega = 2\pi \times 1000$ Hz *vs.* cell width *d*. Red circles and dashed fit are for the left handed cell and blue squares and solid fit for the right handed cell. Error bars for e_c are shown; uncertainty in *d* is approximately the size of the symbols. Each cell may have a small systematic error due to the uncertainty in θ_0. Inset: Relative phase of ac signal for left-and right-handed cells at $d \sim 8.1 \pm 0.2$ and 8.5 ± 0.2 µm, respectively, showing a phase difference of approximately π.

References

---

1. J. Cheng and R.B. Meyer, Phys. Rev. Lett. **29**, 1240 (1972)

2. R.B. Meyer, L. Liebert, L. Strzelecki, and P. Keller, J. Phys. Lett. (Paris) **36**, L69 (1975)

3. N.A. Clark and S.T. Lagerwall, Appl. Phys. Lett. **36**, 899 (1980)

4. See N.A. Clark and S.T. Lagerwall, **Ferroelectric Liquid Crystals**, Gordon + Breach, Philadelphia (1991)

5. L.Komitov, B. Helgee, J. Felix, and A. Matharu, Appl. Phys. Lett. **86**, 023502 (2005)

6. H. Baessler and M. M. Labes, J. Chem. Phys. **52**, 631 (1970)

7. T. Nakagiri, H. Kodama, and K.K. Kobayashi, Phys. Rev. Lett. **27**, 564 (1971)

8. P.G. DeGennes and J. Prost, **The Physics of Liquid Crystals**, Clarendon, Oxford 91994)

9. S. Garoff and R.B. Meyer, Phys. Rev. Lett. **38**, 848 (1977)

10. Z. Li, R.G. Petschek, and C. Rosenblatt, Phys. Rev. Lett. **62**, 796 (1989)

11. S. Ferjani, Y. Choi, J. Pendery, R.G. Petschek, and C. Rosenblatt, Phys. Rev. Lett. **104**, 257801 (2010)

12. J. E. Maclennan, D. Muller, R.-F. Shao, D. Coleman, D.J. Dyer, D.M. Walba, and N.A. Clark, Phys. Rev. E **69**, 061716 (2004)

13. G. Andersson, I. Dahl, P. Keller, W. Kuczynski, S.T. Lagerwall, K. Skarp, and B. Stebler, Appl. Phys. Lett. **51**, 640 (1987)

14. I.M. Syed and C. Rosenblatt, Phys. Rev. E **67**, 041707 (2003); the form used herein has a corrected sign.

15. M. Vilfan and M. Čopic, Phys. Rev. E **68**, 031704 (2003)

16. Z. Li, R. Ambigapathy, R.G. Petschek, and C. Rosenblatt, Phys. Rev. A **43**, 7109 (1991)

17. P.J. Flanders, Mol. Cryst. Liq. Cryst. **29**, 19 (1974)

18. M. R. Wilson and D. J. Earl, J. Mat. Chem.. **11**, 2672 (2001).

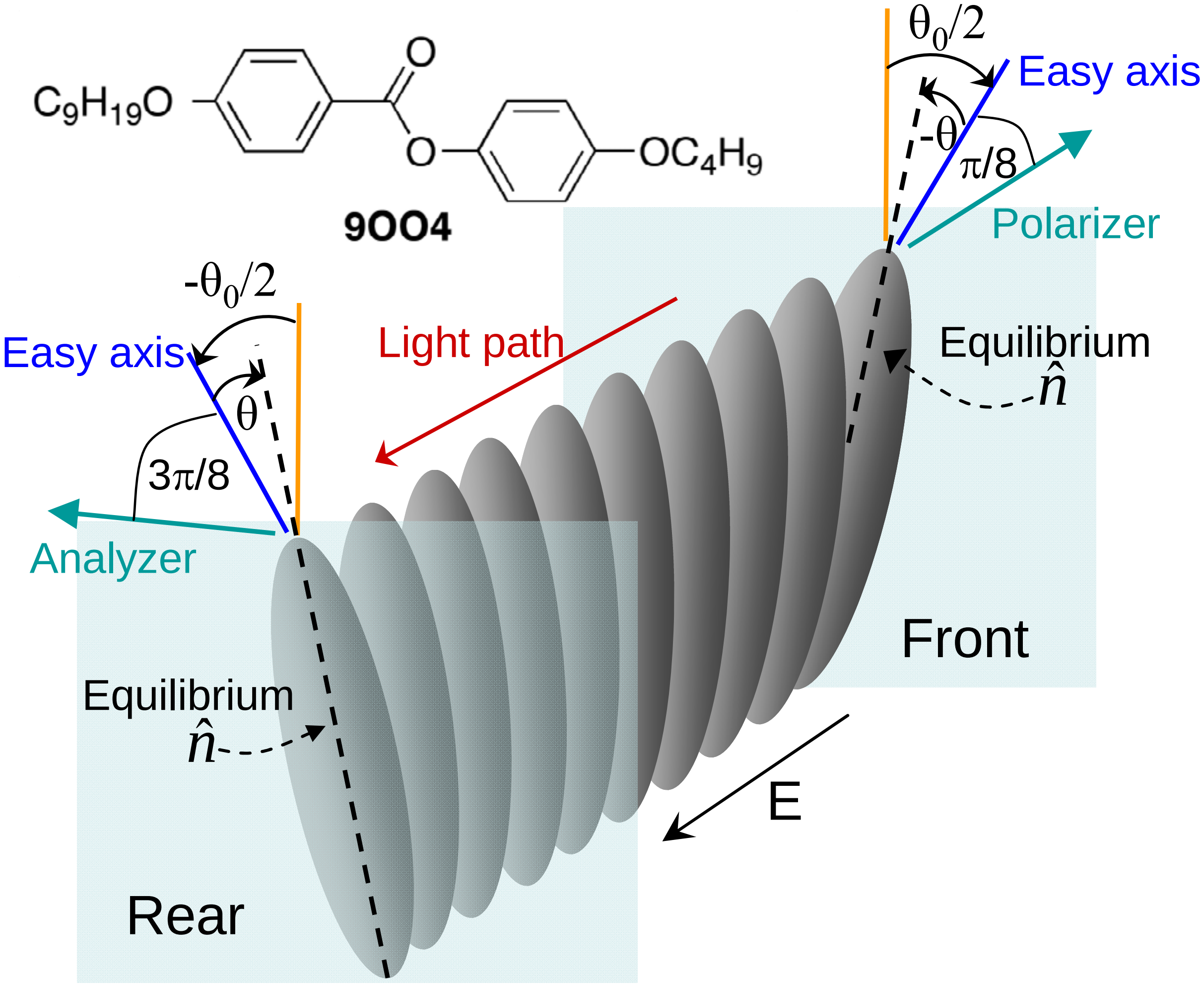

9OO4

$C_9H_{19}O$
O
O
OC_4H_9
$\theta_0/2$
Easy axis
$-\theta$
$\pi/8$
Polarizer
$-\theta_0/2$
Easy axis
Light path
θ
$3\pi/8$
Analyzer
Equilibrium $\hat{n}$
Equilibrium $\hat{n}$
Front
Rear
E

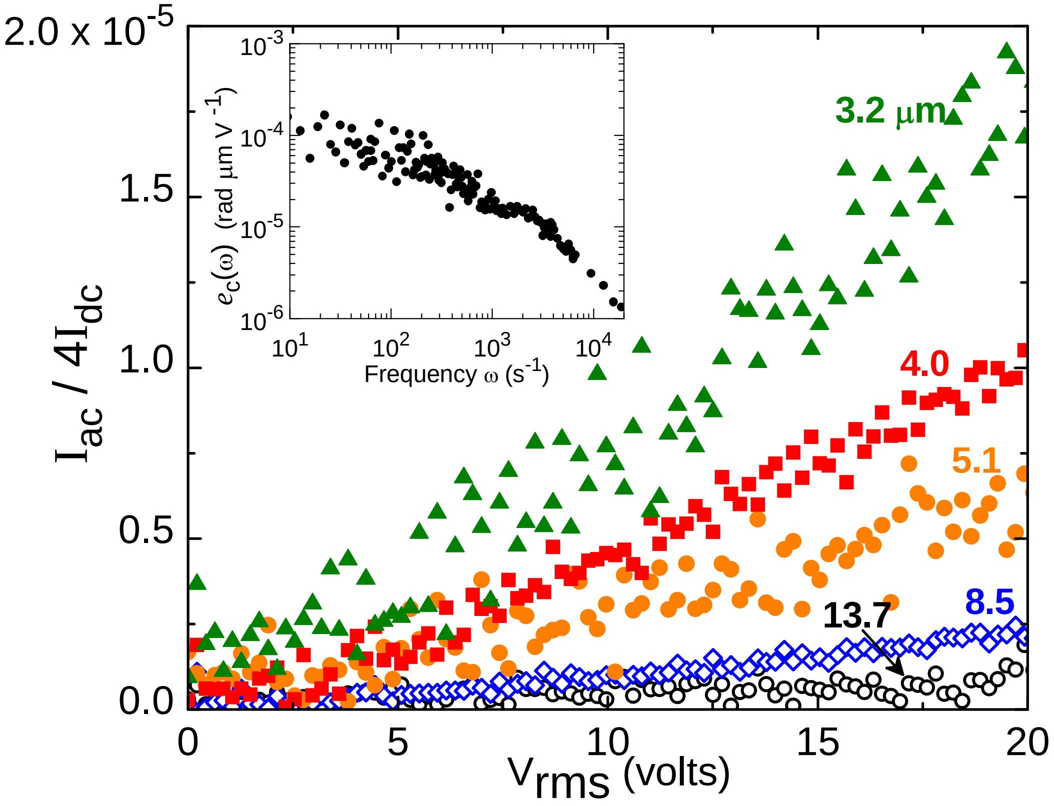
2.0 x 10^-5
1.5
1.0
0.5
0.0
I_ac / 4I_dc
0
5
10
15
20
V_rms (volts)
3.2 μm
4.0
5.1
8.5
13.7
10^-3
10^-4
10^-5
10^-6
e_c(ω) (rad μm V^-1)
10^1
10^2
10^3
10^4
Frequency ω (s^-1)

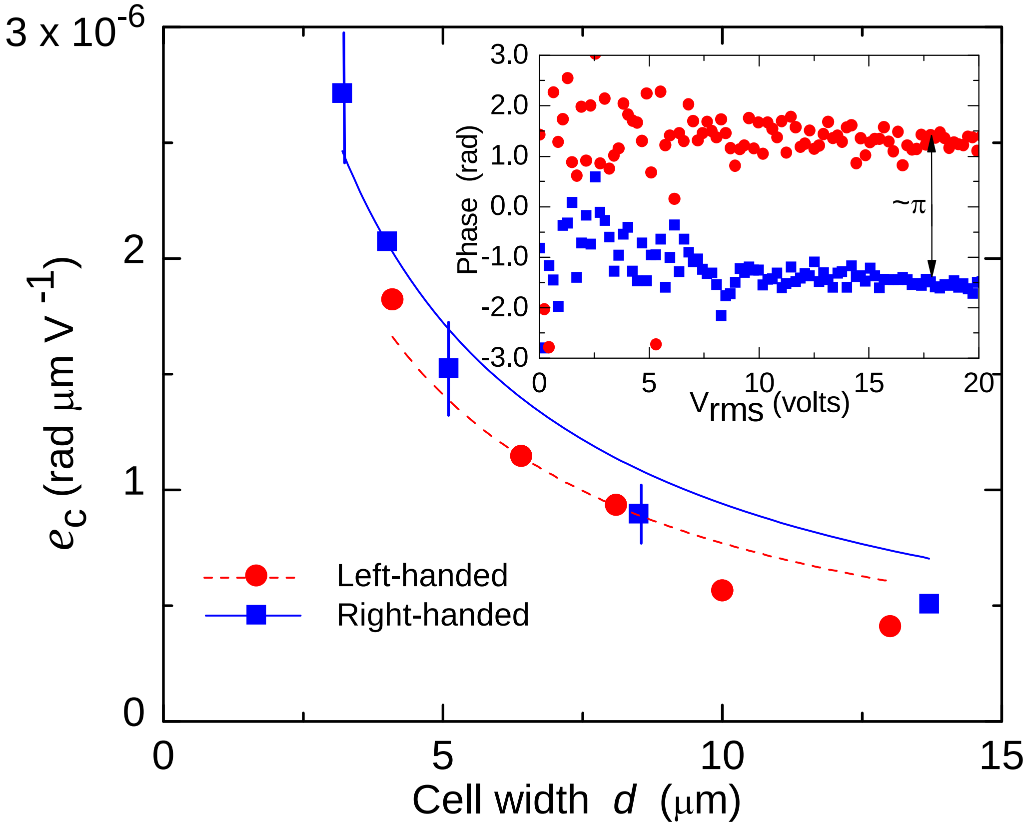
3 x 10^{-6}
2
1
0
e_c (rad µm V^{-1})
0
5
10
15
Cell width d (µm)
Left-handed
Right-handed
3.0
2.0
1.0
0.0
-1.0
-2.0
-3.0
Phase (rad)
0
5
10
15
20
V$_{rms}$ (volts)
~π